

Dynamic Features of Superfluid Turbulence near the Second Critical Heat Current

C. P. Lorenson, D. Griswold, V. U. Nayak,^(a) and J. T. Tough
Department of Physics, The Ohio State University, Columbus, Ohio 43210

(Received 15 July 1985)

Although our understanding of superfluid turbulence has increased dramatically, the nature of the continuous transition at the second critical heat current remains a mystery. We report the first measurements of fluctuations in the dissipation near this transition. The fluctuations appear as broad-band noise without sharp spectral features. A most striking aspect of the data is the structure present in the noise-power amplitude. The results suggest that superfluid turbulence may be a unique system in which to study dynamical transitions.

PACS numbers: 67.40.Vs, 05.40.+j, 05.70.Jk, 47.25.Mr

When a heat current \dot{Q} is passed through a tube filled with He II the dissipation is observed to evolve through three stages as \dot{Q} is increased.¹ For sufficiently low \dot{Q} the only dissipation is that due to the normal-fluid viscosity. At a critical heat current \dot{Q}_{c1} there is a discontinuous transition to a state T-I of larger dissipation associated with the onset of superfluid turbulence. At a larger critical heat current \dot{Q}_{c2} there is a continuous transition to a state T-II of yet larger dissipation and increased turbulence. Our current theoretical understanding of superfluid turbulence is based on the Schwarz theory of a homogeneous distribution of quantized vortex lines in the superfluid.² This theory gives an excellent description of the state T-II³ but as yet has provided no basis for understanding of the T-I to T-II transition. Virtually the only experimental data concerning this transition consist of measurements of \dot{Q}_{c2} as a function of temperature T and tube size. In this paper we provide the results of the first measurements of fluctuations in the dissipation near \dot{Q}_{c2} . The power spectra of the fluctuations contain no sharp lines that would indicate preferred frequencies, but instead are characteristic of broad-band noise. While the frequency dependence of the fluctuations is rather featureless, the dependence on heat current is quite spectacular. The noise-power amplitude varies by two orders of magnitude in a narrow region around \dot{Q}_{c2} . This variation shows a structure far more complex than a simple divergence.

To measure the dissipation we have employed a "chemical potential gradiometer" similar to that described by Yarmchuk and Glaberson.⁴ The apparatus is shown schematically in Fig. 1. The flow tube is glass with diameter $d = 1.34 \times 10^{-2}$ cm and length $l = 1$ cm. The short length of the tube serves to emphasize the local fluctuations in the dissipation at the expense of reducing the steady-state chemical-potential difference. One end of the tube is connected to a ⁴He reservoir regulated at 1.6 K (to $\pm 10 \mu\text{K}$) and the other end to a very low-volume heater chamber. A small-diameter capillary connects this chamber to a differen-

tial pressure transducer through a Vycor-glass superleak. The superleak insures a chemical-potential "short" and provides negligible heat flow from the chamber. The transducer is of the stretched-Mylar-membrane type discussed by Landau *et al.*,⁵ except that the body is oxygen-free high-conductivity copper. A wide tube connects the bottom side of the transducer to the reservoir. The transducer is thermally anchored to the reservoir, thus assuring that the pressure difference across the transducer is proportional to the chemical-potential difference $\Delta\mu$ across the flow tube. The pressure difference is detected by measurement of the change in capacitance ΔC between the gold-covered membrane and a fixed plate in the body of the transducer. Using a capacitance bridge we measure the average value $\langle \Delta C \rangle$ and calculate the steady-state chemical-potential difference $\langle \Delta\mu \rangle$. Fluctuations in

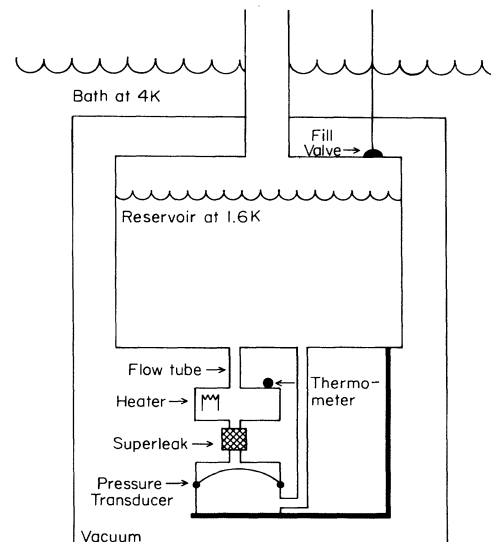


FIG. 1. Schematic drawing of the apparatus. The thick line between the transducer and the reservoir represents the thermal anchor.

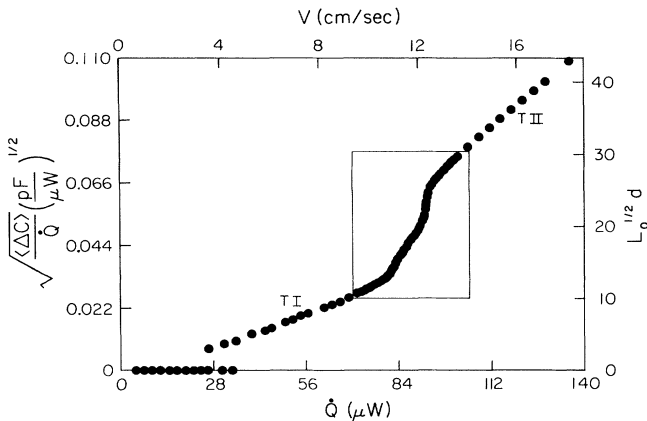


FIG. 2. The steady-state dissipation as a function of the heat current \dot{Q} showing the T-I to T-II transition. The chemical-potential difference across the flow tube $\langle \Delta\mu \rangle$ is proportional to $\langle \Delta C \rangle$, and $(\langle \Delta C \rangle / \dot{Q})^{1/2}$ is proportional to the dimensionless vortex line density $L_0^{1/2}d$ shown on the right-hand scale. The upper scale gives the relative velocity between the normal fluid and the superfluid. The boxed region in the figure is enlarged in Fig. 3.

the chemical potential $\delta\mu$, where

$$\Delta\mu = \langle \Delta\mu \rangle + \delta\mu(t), \tag{1}$$

are analyzed by passing the off-balance signal from the capacitance bridge through suitable electronics to a computer. We were able to resolve $\langle \Delta\mu \rangle$ to about three parts in 10^5 . The sensitivity of the gradiometer is sufficient to detect fluctuations in the chemical potential equal to 0.5% of the steady-state value $\langle \Delta\mu \rangle$.

Figure 2 shows our data for the steady-state chemical-potential difference as a function of the heat current \dot{Q} . To compress the dynamic range of the data we plot $(\langle \Delta C \rangle / \dot{Q})^{1/2}$. This quantity can be directly

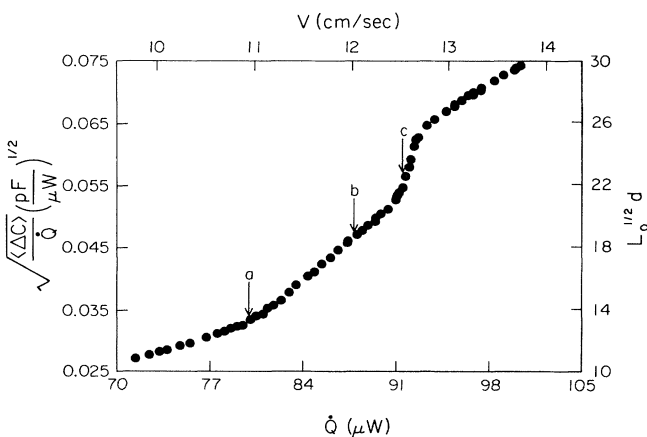


FIG. 3. The steady-state dissipation as a function of the heat current \dot{Q} in the T-I to T-II transition region shown in Fig. 2. The points labeled a, b, and c refer to Figs. 4 and 5.

related to the vortex line density L_0 if the superfluid turbulence can be regarded as homogeneous. In that case the simple mutual-friction model gives

$$L_0^{1/2} = K (\langle \Delta C / \dot{Q} \rangle)^{1/2}, \tag{2}$$

where K is a constant that depends on the transducer calibration and properties of the He II. The right-hand scale of Fig. 2 gives the dimensionless vortex line density $L_0^{1/2}d$ and the upper scale gives the relative velocity V between the superfluid and the normal fluid, proportional to the heat current \dot{Q} .

The data in Fig. 2 are typical of previous low-resolution measurements of the dissipation in thermal counterflow,⁶⁻¹⁰ showing a nonturbulent region where $L_0=0$, the state T-I, and a rather broad continuous transition to the state T-II. The sensitivity of our chemical-potential gradiometer allows a much more detailed examination of the T-I to T-II transition. Data from the boxed region in Fig. 2 are shown in Fig. 3 and reveal a new and rather complex structure for the transition. It is not at all clear from these data how the "critical heat current" \dot{Q}_{c2} is to be identified.

Our initial analysis of the fluctuations in the chemical potential $\delta\mu$ consisted of a determination of the distribution of amplitudes and the power spectrum $P(f)$ of the fluctuations. The amplitude distribution was found to be nearly Gaussian in every case. Power spectra obtained at four different heat currents are shown in Fig. 4, with labels referenced to the steady-state data of Fig. 3. The background noise (mainly due to the temperature regulation) is shown as the open circles. The spectra indicate a broad-band noise of approximately the same frequency dependence but with an *amplitude* that grows dramatically and then decays again as the T-I to T-II transition has evolved. Previous measurements of fluctuations associated with

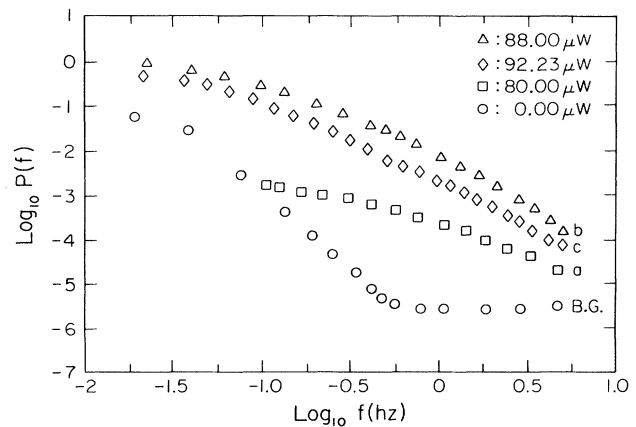


FIG. 4. The power spectra of the chemical-potential fluctuations at three different heat currents (points a, b, and c of Fig. 3). The low-frequency rise of the background ($\dot{Q} = 0$) spectrum is due to the temperature regulation.

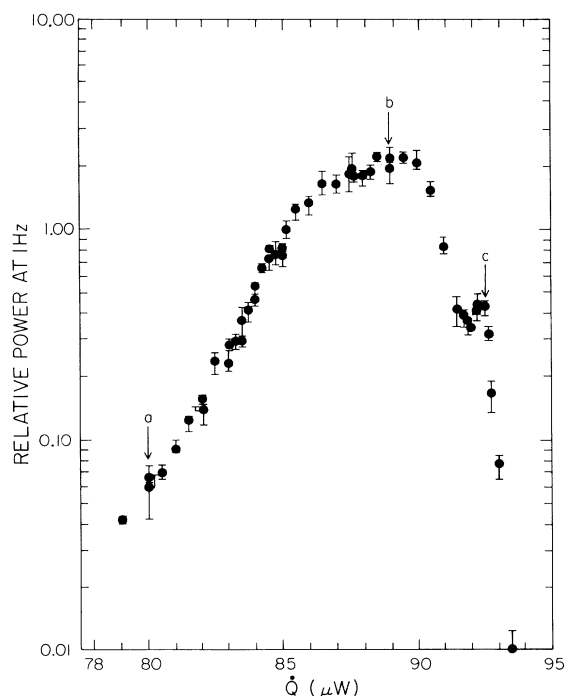


FIG. 5. The relative power at 1 Hz as a function of the heat current. The points a, b, and c refer to Figs. 3 and 4. The error bars represent the spread in the data at each heat current.

superfluid turbulence¹¹⁻¹⁴ have shown a rather flat low-frequency spectrum with a rapid rolloff at high frequencies. Smith and Tejwani¹⁴ have demonstrated that the high-frequency dependence is $1/f^4$. These previous data were all obtained with flow tubes several orders of magnitude larger than in the present experiment. In such large tubes only the state T-II is observed, and the fluctuations are thus representative of the dynamics of that state. Our data are the first to reveal the structure of the fluctuations near the T-I to T-II transition. Clearly the most dramatic feature of our measurements is the dependence of the power amplitude on heat current \dot{Q} .

In order to explore this dependence we have measured the amplitude of the power spectrum as a function of the heat current \dot{Q} at a fixed frequency f_0 . The results given in Fig. 5 were obtained with a filter having a center frequency f_0 of 1.0 Hz and a 18-dB/octave high- and low-frequency rolloff. The power amplitude in Fig. 5 shows a remarkably complex structure, including a narrow peak in the power at point c. Similar results are obtained with use of $f_0 = 0.63$ and 0.1 Hz. The points labeled a, b, and c in Fig. 5 are also located in the steady-state data of Fig. 3 and correspond to the heat currents for the power spectra in Fig. 4. The power spectra between points a and c show no substantial change in frequency dependence. The maximum

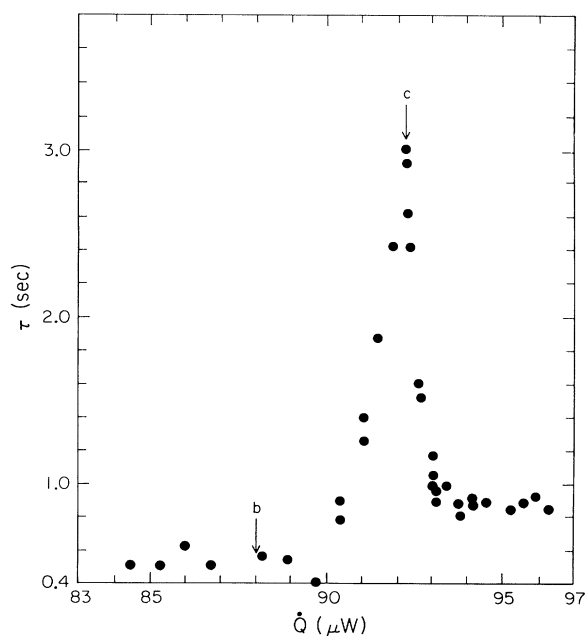


FIG. 6. The exponential response time τ as a function of heat current for a small region around the T-I to T-II transition. The points b and c refer to Figs. 3, 4, and 5.

power amplitude at point b does not correspond to any particularly notable feature in the steady-state data. The well-resolved peak in the amplitude at point c, however, does correspond to the maximum slope in the steady-state data.

Several previous experiments^{7,8} have shown a dynamic effect similar to "critical slowing down" near the T-I to T-II transition and we have repeated these experiments with our apparatus in order to associate this effect with the structure shown in the power-amplitude data (Fig. 5). The heat current is stepped from a value \dot{Q} to $\dot{Q} + \delta\dot{Q}$ (where $\delta\dot{Q}/\dot{Q} \leq 0.4\%$) and the time response of the resulting chemical-potential difference is analyzed. As a result of the large fluctuations, a substantial amount of signal averaging is required to determine the exponential response time τ . The results are given in Fig. 6, and show a pronounced peak in the response time at a heat current corresponding to the narrow peak in the power amplitude, point c.

It should be noted that the experiments reported here represent one of the very few *direct* observations of fluctuations near a continuous transition. Although the field of light scattering near a critical point is based upon the existence of such fluctuations, there appear to be only a few^{15,16} direct experimental observations. In the case of nonlinear dynamical systems, Moss¹⁷ has recently observed an increased noise level near the transition in an analog simulation. (Sancho *et al.*¹⁸ have also recently reported a strong increase in the

response time at the transition in this system.) Donnelly *et al.*¹⁹ have directly observed an increase in broad-band noise near a hydrodynamic transition. If we consider the relative ease with which the fluctuations in superfluid turbulence can be observed, and the rich dynamical structure revealed, this system may prove to be a unique one for the study of continuous transitions.

Our experiments have revealed for the first time the large fluctuations associated with the T-I to T-II transition in superfluid turbulence. The power spectra of the fluctuations are characteristic of broad-band noise showing no evidence of fluctuations at preferred frequencies. The noise-power amplitude increases dramatically at the transition and its variation with heat current reveals a strikingly complex structure. We have shown that several features of this structure can be associated with features in the average dissipation. A narrow peak in the power amplitude is shown to correspond to the heat current at which the system response time appears to diverge.

This work has been supported by the National Science Foundation, Low-Temperature Physics Program, Grant No. DMR8218052.

^(a)Presently at IBM, San Jose, Cal. 95193.

¹J. T. Tough, in *Progress in Low-Temperature Physics*, edited by D. F. Brewer (North-Holland, Amsterdam, 1982), Vol. 8, Chap. 3.

²K. W. Schwarz, *Phys. Rev. Lett.* **49**, 283 (1982).

³D. D. Awschalom, F. P. Milliken, and K. W. Schwarz, *Phys. Rev. Lett.* **53**, 1372 (1984).

⁴E. J. Yarmchuk and W. I. Glaberson, *J. Low Temp. Phys.* **36**, 381 (1979).

⁵J. Landau, J. T. Tough, N. R. Brubaker, and D. O. Edwards, *Rev. Sci. Instrum.* **41**, 444 (1970).

⁶D. F. Brewer and D. O. Edwards, *Philos. Mag.* **7**, 721 (1962).

⁷D. R. Ladner, R. K. Childers, and J. T. Tough, *Phys. Rev. B* **13**, 2918 (1976).

⁸K. P. Martin and J. T. Tough, *Phys. Rev. B* **27**, 2788 (1983).

⁹R. P. Slegtenhorst, G. Marees, and H. van Beelen, *Physica (Amsterdam)* **B113**, 341 (1982).

¹⁰G. Marees and H. van Beelen, *Physica (Amsterdam)* **B** (to be published).

¹¹H. Hoch, L. Busse, and F. Moss, *Phys. Rev. Lett.* **34**, 384 (1975).

¹²J. Mantese, G. Bischoff, and F. Moss, *Phys. Rev. Lett.* **39**, 565 (1977).

¹³R. M. Ostermeier, M. W. Cromar, P. Kittel, and R. J. Donnelly, *Phys. Lett.* **77A**, 321 (1980).

¹⁴C. W. Smith and M. J. Tejwani, *Phys. Lett.* **104A**, 281 (1984).

¹⁵J. J. Brophy and S. L. Webb, *Phys. Rev.* **128**, 584 (1962).

¹⁶M. W. Kim, Y. C. Chou, W. I. Goldberg, and A. Kumar, *Phys. Rev. A* **22**, 2138 (1980).

¹⁷F. Moss, private communication.

¹⁸J. M. Sancho, R. Mannella, P. V. E. McClintock, and Frank Moss, *Phys. Rev. A* (to be published).

¹⁹R. J. Donnelly, K. Park, R. Shaw, and R. W. Walden, *Phys. Rev. Lett.* **44**, 987 (1980).